Article

Adaptive Volt-VAr control algorithm to grid strength and PV inverter characteristics

Toni Cantero Gubert [1,*], Alba Colet Subirachs [1], Lluc Canals Casals [1], Cristina Corchero [1], José Luis Domínguez-García [1], Amelia Alvarez de Sotomayor [2], William Martin [3], Yves Stauffer [3] and Pierre-Jean Alet [3]

[1] Catalonia Institute for Energy Research (IREC), Sant Adrià de Besòs (08930), Spain
[2] Schneider Electric, Sevilla (41092) Spain
[3] Swiss Center for Electronics and Microtechnology (CSEM), Neuchâtel (2002), Switzerland
* Correspondence: tcantero@irec.cat

Abstract: High-penetration of Distributed Energy Resources (DER) in low voltage distribution grids, mainly photovoltaics (PV), might lead to overvoltage in the point of common coupling. Volt-VAr is one of the common control functions for DER power converters used to enhance the stability and the reliability of the voltage in the distribution system and, thus, fulfilling the network operator requirements. In this study, a centralized algorithm will provide local Volt-VAr control parameters to each PV inverter, based on the electrical grid characteristics where each equipment is installed. Since accurate information of grid characteristics is typically not available, the parametrization of the electrical grid is done using power meter data in DER location and a voltage sensitivity matrix. The algorithm has different optimization modes to both minimize voltage deviation and line current. In order to validate the effectiveness of the algorithm and its deployment in real infrastructure, it has been tested in an experimental setup with PV emulators in a set of 5-day tests. Volt-VAr control algorithm successfully adapted its parameters based on grid topology and PV inverter characteristics, achieving a voltage reduction up to 25% of the allowed voltage deviation.

Keywords: Distributed power generation; low-voltage; test facilities; standards; voltage regulation; reactive power; microgrids; photovoltaic systems; optimization methods

1. Introduction

Distributed Energy Resources (DER), such as photovoltaic (PV) systems, are increasingly being integrated into distribution network due to low carbon emission, affordable price at small-scale level and technology maturity as a strategy to face climate change [1]. It exists several technical problems for massive DER deployment, such as harmonics distortion, reverse power flows, power losses, etc.[2]. Among them, overvoltage is the main potential problem at the distribution level [3]. Several strategies to correct voltage deviation and enhance grid stability exist, such as line refurbishing, on-load tap changers (OLTC), capacitor banks and static VAr compensators, battery storage, demand-size management and line voltage regulators among others [4]. While most of the previous solutions are either expensive or difficult to integrate, a more efficient and economical solution is the usage of the capabilities of the power electronics of PV inverters for network stability [5]. Standards such as EN 50438 and national grid codes allows grid-tied PV inverters to participate actively in voltage regulation adjusting the exchange of reactive power [6]. However, it is the compliance of standard EN 50160 [7], which indicates the maximum permissible voltage deviation at the Point of Common Coupling (PCC), the one that would point out the maximum integration of DER. By absorbing or injecting reactive power, it is possible for a smart inverter to correct an over or under voltage.

Voltage regulation is highly dependent on the grid topology where the generation devices are placed [8] so a solution to increase the penetration of renewables have to consider the grid characteristics where the DER are installed. The resistance (R) and the reactance (X) of the power cables together with the short circuit ratio (SCR) are the indicators that define the grid strength, i.e., the ability of the grid to maintain its voltage constant during the injection of active and reactive power from an energy source. *SCR* and *X/R* ratio are the

Preprints (www.preprints.org) | NOT PEER-REVIEWED | Posted: 26 February 2021 doi:10.20944/preprints202102.0595.v1

main indicators on grid strength [9].
The expression in 1 relates the voltage deviation from the PV inverter in the PCC (U_{PCC}) to the voltage source (U_G) with the grid resistance (R), reactance (X) and the amount of injected active power (P) and reactive power (Q) by the DER. It is used to see the overvoltage effect of a single DER to the distribution grid, taking into account grid characteristics.

$$\Delta\vec{U} = \vec{U_{PCC}} - \vec{U_G} \approx (R \blacksquare P + X \blacksquare Q)/U_{PCC} \quad (1)$$

As seen in equation 1, X and R values will play an important role on the effectiveness of this method. A Volt-VAr control technique is used to adjust the amount of reactive power based on the voltage level at PCC, so more reactive power is absorbed when voltage deviation is bigger. In [10], it is proved its effectiveness in front other techniques.
Following the standard IEC 61850-90-7 and as it is mentioned in [11] and [12] the Volt-VAr function can be managed by either an autonomous DER unit itself responding to local conditions or broadcasted from a centralized power system provider with the ability to understand the capacities of each individual DER. Meanwhile a centralized control can gather the processing capabilities in a central equipment, a local control is able to work when there is communication problem with the centralized system.
In our study, the usage of Remote Terminal Units (RTU) will allow both a local or centralized control; acting as gateway for each individual PV inverter and a centralized system provider that pictures the whole grid. RTUs are commonly used to transmit data from electrical substations or remote areas to distributed control systems and at the same time, they have processing capabilities to host algorithms and act locally.
In [13], an adaptive reactive power control is proposed but the control parameters are the same for each PV inverter in order to distribute the power demand so it is not adapted to each unit. However, in our study, a RTU is installed close to the PCC obtaining local measurements and providing the parameters that define the Volt-VAr control to each PV inverter; this versatile equipment gives a clear advantage in front of what is exposed.
Meanwhile in [14] new requirements for Volt-VAr control functions are highlighted, such as the minimization of line losses, in our study this requirement is included and extended with an algorithm design that is able to adapt the control parameters to the grid topology changes. Its unique feature makes this algorithm valuable since it is a global solution for both weak and strong grids.
In [15] the effectiveness of updating the parameters of Volt-VAr control is proven depending on the amount of PV penetration and weather which is also considered in our study where the algorithm delivers optimized parameters based on the inverter size with the aim to reduce voltage deviation.
While most of the studies rely only on simulation results [10] [14], a step forward has been implemented in this work by doing experimental tests in order to prove the effectiveness of the algorithm in controlled conditions for 5-day in laboratory tests emulating real conditions. A simplified system consisting on a grid emulator, a PV inverter and an impedance is used in a microgrid laboratory to study the influence of a reactive power control algorithm in a power system without loads. This simplified representation of a power system in a two-bus equivalent model proved to be accurate when estimating the overvoltage impact due to PV across a distribution network [16].
Different approaches exist when defining the strategy of the algorithm design, in [17] an artificial neural network control is proposed to understand the reaction of DER inverters, in our study, though, it is used real power meter data to train the sensitivity matrix that will describe the network behavior using heuristic optimization methods.

The main contributions of this paper are:

- A new algorithm that adapts the Volt-VAr parameters to different network conditions (strong or weak grids) and PV inverter characteristics based on power meter data with the aim to reduce overvoltage and line loading

Preprints (www.preprints.org) | NOT PEER-REVIEWED | Posted: 26 February 2021 doi:10.20944/preprints202102.0595.v1

- The validation of its effectiveness in a laboratory with real equipment and with communication elements such as RTUs, being a bridge from simulation environments to a large-scale deployment.

This work has been carried under the project SABINA (SmArt Bi-directional multi eNergy gAteway), grant agreement 731211. The European Community Horizon 2020 program has financially supported this research.

2. Materials and Methodology

2.1. Adaptive Volt-VAr control algorithm

The Volt-VAr control function consists of five parameters whose representation will draw the curve shown in Figure 1. Q_{max} and Q_{min} are the reactive power capabilities of the inverter or the limits imposed by the manufacturer. u_{min} and u_{max} determine the dead-band where the reactive power is not exchanged and d is the droop parameter that corresponds to the slope of the curve. Being u_{meas} the voltage measured at the PCC expressed in per unit (pu) and S_{nom} the total apparent power of the inverter, the resulting reactive power can be computed as follows (equations 2 and 3):

$$Q_{inj\,or\,abs} = 100 \blacksquare (u_{min\,or\,max} - u_{meas}) \blacksquare S_{nom}/d, \tag{2}$$

$$Q_{max} \leq Q_{inj\,or\,abs} <= Q_{min}, \tag{3}$$

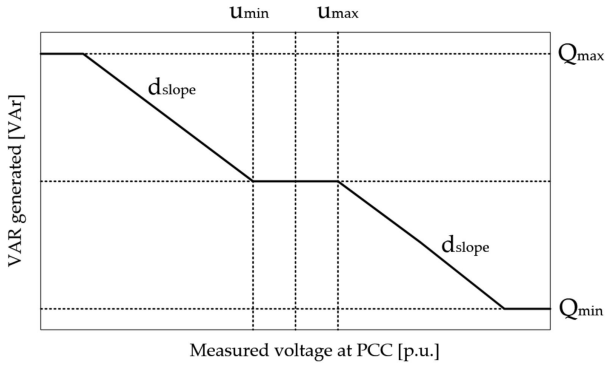

Figure 1. Q(u) curve of Volt/VAr control: reactive power absorbed or injected as a function of the measured voltage in the PCC

A new algorithm has been developed by CSEM to find out the optimal parameters of Volt-VAr controllers based on power meter data [18]. The aim of the algorithm consists on finding these optimal parameters independently of a simulation program that represents the electrical grid, which requires detailed information of the network where the PV systems are located and this information is usually not available or accessible. For that reason, a voltage sensitivity matrix is used to represent an approximation of the grid topology without the need of exact network details. The voltage sensitivity matrix is derived from the power flow equations 4 and 5: P_i is the measured active power at node i, Q_i the reactive power, U_i the voltage, G_{ij} is the real part of the admittance of the line connecting node i to node j, B_{ij} is the imaginary part of the admittance and finally θ_i is the voltage phase of node i.

$$P_i = U_i \sum_{j=1}^{n} U_j (G_{ij} cos(\theta_i - \theta_j) + B_{ij} sin(\theta_i - \theta_j)), \tag{4}$$

$$Q_i = U_i \sum_{j=1}^{n} U_j (G_{ij} sin(\theta_i - \theta_j) + B_{ij} cos(\theta_i - \theta_j)) \tag{5}$$

Preprints (www.preprints.org) | NOT PEER-REVIEWED | Posted: 26 February 2021 doi:10.20944/preprints202102.0595.v1

Voltage sensitivity matrix is a known method described in [12] [19] [20]. The matrix computation allows to predict the change in voltage if measurements of power are available, which can be easily be obtained with basic metering equipment.

The implementation strategy of the algorithm consists of four steps:

1. Training period: It consists on training the sensitivity matrix, setting non-optimal control parameters and recording the voltage, the active and reactive power. The Volt-VAr parameters will vary randomly every minute in a range of reasonable values, trying to represent an average standard parametrization. It lasts 2 days with measurements every minute, having a total of 2880 points.
2. Reference scenario: It consists on turning off the Volt-VAr controllers and measure the voltage, the active and reactive power with the aim of comparing these values with the scenario with optimal parameters. It lasts 5 days with measurements every minute, having a total of 7200 points. Even though the active and reactive power are known parameters imposed to the PV emulator, a mismatch exists between the imposed values and the real ones as mentioned in the discussion section.
3. Offline optimization: It consists on a Black box optimization from an initial set of Volt-VAr parameters (simplex Xk). A Nelder-mead algorithm, which is able to evaluate n-different initial points by n-simplex, proposes new parameters until the optimal is found. The cost function here is a trade-off between minimizing the voltage deviation and the line current increase [18].
4. Evaluation period: It consists on the implementation of the optimal parameters found by the algorithm in step 3 to the PV inverter. It lasts 5 days with measurements every minute, having a total of 7200 points.

In section 3.1, a flowchart is presented with the four steps of the implementation strategy together with other relevant data for the experiment definition.

2.2. Two-Bus Equivalent Model

An experimental validation with actual PV inverters is a demand from previous studies, not only for their performance but also for the integration with the communication devices (such as RTUs) and as a previous step for a deployment at larger-scale as it is planned in the scope of SABINA project. Then, in order to test the effectiveness of the reactive power control algorithm in a physical and controlled environment some simplifications have to be done in terms of LV network representation. A simplified model is used to estimate accurately the magnitude of overvoltage within LV areas with limited data in a small amount of time. Such data is limited to the impedance of each branch and the parent branch, to which they are connected, as well as the load/generator ratings and parent connection. In that way, the LV area can be represented by two-bus model comprised of three components: a slack bus with a defined reference voltage, an equivalent network impedance and a PQ bus for the PV generation. As shown in Figure 2, bus B_0 is the slack bus, representing the connection of the grid at a fixed reference voltage U_G. Bus B_1 connects the PV generation (S_{PV}) to the grid through an equivalent impedance (Z_{eq}). U_{PCC} will be the maximum voltage in the LV area during the tests representing the furthest point from the voltage source.

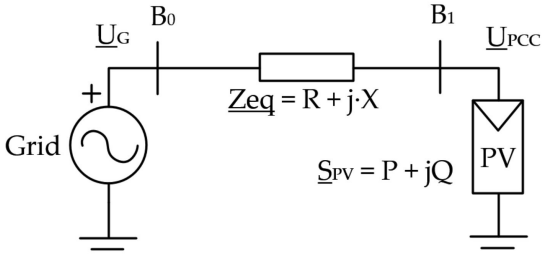

Figure 2. Two-bus equivalent model of a full network after reduction

Preprints (www.preprints.org) | NOT PEER-REVIEWED | Posted: 26 February 2021 doi:10.20944/preprints202102.0595.v1

From the previous representation and assuming a small variation in the angle between U_G and U_{PCC}, equation 1 is obtained. The two-bus model is very useful to prepare the tests in the microgrid laboratory and to link the grid topology up with the inverter size and location. Considering the nominal voltage at which the reference voltage is imposed (U_G), the total apparent power of the inverter (S_{PV}) together with the common indicators of grid characteristics (SCR and X/R ratio) , the relation of the total equivalent resistance (R) and reactance (X) as a function of the previous four indicators is found. The development of equations 8 and 9 comes from the definition of the SCR (equation 6), as the ratio between the short circuit capacity (SCC) of the grid and the rated power of the energy source (S_{PV}). Equation 7 relates the equivalent impedance with X/R ratio (xrr):

$$SCR = SCC/S_{PV} = U_G/(|Z_{eq}|\blacksquare S_{PV}]) \tag{6}$$

$$|Z_{eq}| = \sqrt{R^2 + X^2} = R\sqrt{(1 + xrr^2)} = X\sqrt{(1 + xrr^{-2})} \tag{7}$$

$$R = (U_N^2 \blacksquare \sqrt{1 + xrr^2})/(SCR \blacksquare S_{PV}) \tag{8}$$

$$X = (U_N^2 \blacksquare \sqrt{1 + xrr^{-2}})/(SCR \blacksquare S_{PV}) \tag{9}$$

The previous equations are used to define the resistance and reactance values of the test design section.

2.3. Energy Smart Laboratory

The facilities of the Catalonian Institute for Energy Research (IREC) count with the Energy Smart Laboratory that has a configurable AC three-phase network, which interconnects several power electronics converters, battery storage systems and power load banks. It is based on a hardware emulation approach, which allows for real physical equipment to operate under a broad range of scenarios of real conditions without depending on the boundary conditions of specific equipment, and thus being suitable for experimental validations [21], [22]. For the setup involved in this experiment, there are two main groups of elements:

1. The power electronics system, in figure 3:
   - A grid emulator that acts as voltage source setting up the reference voltage and frequency of the emulated microgrid. In this case, all tests are fixed at 400V and 50Hz.
   - An emulated distribution line consisting on a variable inductance and a resistance that range from 0 to 20 Ohms both the resistance and the reactance.
   - A PV emulator with 4-kVA maximum apparent power operation.

Preprints (www.preprints.org) | NOT PEER-REVIEWED | Posted: 26 February 2021 doi:10.20944/preprints202102.0595.v1

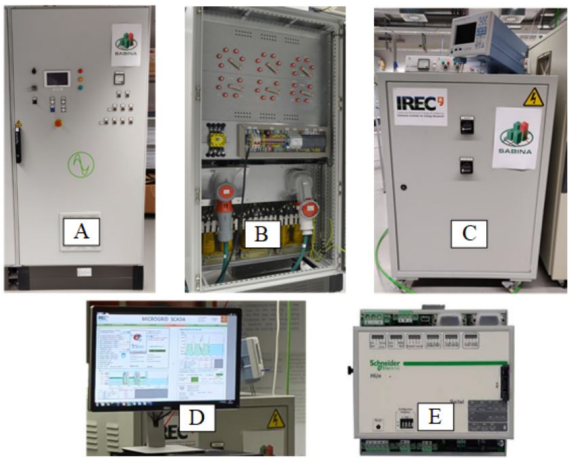

Figure 3. Key components of the experimental setup. A) Grid emulator, B) Line emulator, C) Emulated PV, D) SCADA, E) RTU

2. The control and communications system, in figure 4:
   - A PV emulator adapted to meet the requirement for the study: It calculates the reactive power to absorb based on the parameters of the Volt-VAr curve. It also collects electrical measurements and sends them to the RTU.
   - A Schneider Electric RTU [23] provides the parameters from the Volt-VAr curve once they are calculated depending on the control mode selected by the adaptive algorithm. It might be hosted in the RTU or remotely, if so, the RTU communicates through MQTT to an external server with processing capabilities. A patent in this regard is being published by Schneider Electric.
   - A Supervisory Control and Data Acquisition (SCADA) where the experiments are controlled and the information gathered. It tracks the communication between the RTU and the external server as well.

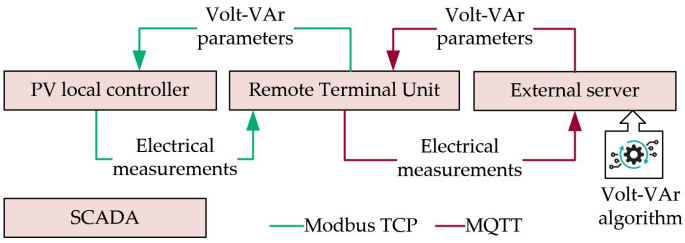

Figure 4. Communication interaction between components. The color of the arrow expresses the protocols used. The algorithm is hosted in an external server

3. Case Study

3.1. Test design

Due to previous considerations and the capabilities of the microgrid laboratory, the tests are designed to evaluate both the effectiveness of the reactive power control and to compare it between different grid topologies and optimization modes. Two scenarios are presented:

- Scenario 1 (S1): Strong grid with short distribution line, this is a grid topology with large SCR and X/R ratio. It represents a scenario where the PV inverter is installed near an electric substation, so it is less sensitive to voltage changes.
- Scenario 2 (S2): Weak grid with large distribution line, this is a grid topology with small SCR and X/R ratio. It represents a scenario where the PV inverter is installed in a remote area, more sensitive to voltage changes.

An X/R ratio of 0.5 is considered to be low enough to represent the weak grid topology of S2, being twice more resistive than inductive. High values of resistance will produce

Preprints (www.preprints.org) | NOT PEER-REVIEWED | Posted: 26 February 2021 doi:10.20944/preprints202102.0595.v1

a voltage rise at PCC that should not exceed the EN 50160 regulation; in order to avoid PV emulator malfunctioning, the maximum resistance in the setup is calculated to not overpass the 10% of nominal voltage in case of maximum power injection. Then, from equation 1, considering S_{PV}=4kW as the maximum rated power of the PV inverter, nominal voltage of U_G=400V and neglecting the effect of reactive power, Q=0VAr P=4000W, the maximum resistance to set in IREC laboratory is 4.4Ω . Taking R=4Ω in order to avoid reaching the limits, the remaining parameters SCR and X are obtained. For the strong grid topology of S1 an X/R ratio of at least 3 is taken in order to have an inductive driven grid and considering that the minimum resistance that can be set in the laboratory has to be at least of 0.7Ω the values for X and SCR are obatined. The resulting parameters are exposed in Table 1:

Table 1. Grid topology parameters defined for each scenario. The imposed parameters are in italics

	SCR ratio	X/R ratio	R [Ω]	X [Ω]
S1	18.1	*3*	*0.7*	2.1
S2	9.0	*0.5*	*4.0*	2.0

A reactance of 2Ω is close to the realistic value for a low voltage distribution grid (0.6 to 3.5 Ω). Those values include the impedance of the transformer and a length of 300m in case of the S1 and 1600m for S2.

The active power injected by the PV emulator follows a pattern obtained from real PV panels and scaled in a way that the maximum power injected is 4000W as this is the limit of PV emulator power in the laboratory (Figure 5). The same 5-day PV production pattern is followed both in reference and evaluation periods. The real data used to train the sensitivity matrix during the training period corresponds to the first 2-days of the same pattern.

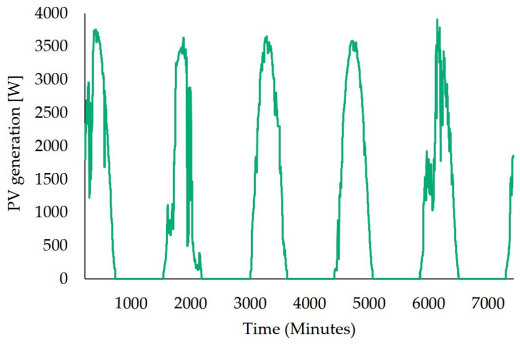

Figure 5. PV generation for a 5-day test. The starting point corresponds to 9am

As mentioned previously, every test consists of four steps: training period, reference period, optimization and evaluation (Figure 6). This flow diagram will be repeated not only for the different scenarios but also for the different optimization modes tested.

Preprints (www.preprints.org) | NOT PEER-REVIEWED | Posted: 26 February 2021 doi:10.20944/preprints202102.0595.v1

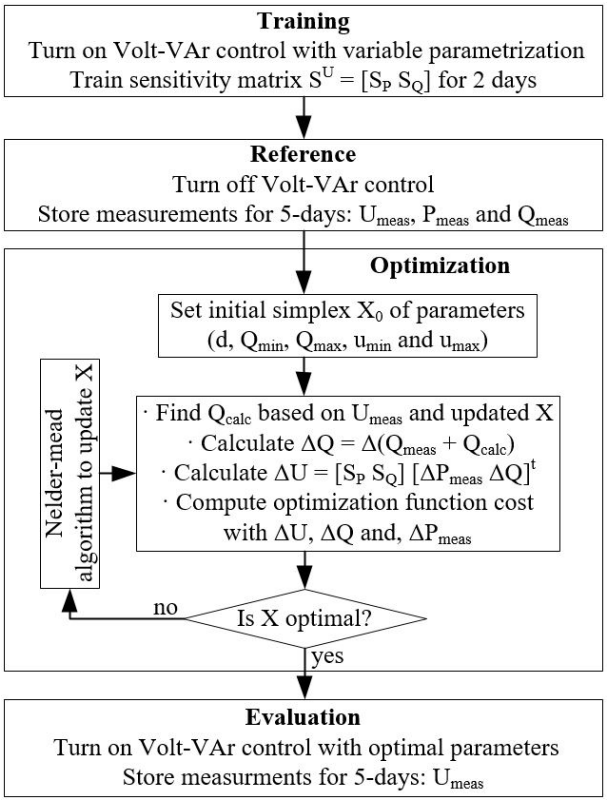

Figure 6. Implementation strategy flowchart

As previously commented when describing the Volt-VAr algorithm, since voltage regulation with reactive power is a trade-off between correcting voltage deviation and the increase of line current, three different optimization modes of balancing these indicators were tested: The *mixed*, the *full voltage* and the *balanced*.

- The *mixed* (M) mode gives the same weight to the cost function to minimize voltage deviation and line current increase.
- The *full voltage* (FV) mode aims to achieve the maximum voltage reduction compared to any of the other control modes.
- The *balanced* (B) mode falls between the *mixed* and the *full voltage* mode giving more importance to the voltage deviation reduction in the cost function compared with the *mixed* mode.

Thus, the testing phase consists of 6 tests as summed up in table 2: 3 tests with S1 and 3 tests with S2 testing all different optimization modes. The reference and the training periods are done only once per scenario, meanwhile the optimization and evaluation period need to be conducted in all 6 tests.

Table 2. Summary of the scenarios, periods and optimization modes carried out in each test

Test	T1	T2	T3	T4	T5	T6
Scenario	1	2	1	2	1	2
Training	x	x				
Reference	x	x				
Optimization	x	x	x	x	x	x
Evaluation	x	x	x	x	x	x
Optimization mode	M	M	FV	FV	B	B

Preprints (www.preprints.org) | NOT PEER-REVIEWED | Posted: 26 February 2021 doi:10.20944/preprints202102.0595.v1

3.2. Key Performance Indicators (KPI)

In order to test the effectiveness of the Volt-VAr parameters found by the adaptive algorithm the reference and evaluation periods are compared for different scenarios and optimization modes. Since the purpose of this study focuses on overvoltage situations, the parameters analyzed in the results section are u_{max}, Q_{min} and droop. The following KPI are highlighted:

- *Droop effectiveness (Volt/Volt)*: It indicates how many Volts the reactive power control is able to reduce compared with the reference period where there is no voltage regulation. The maximum value possible is 1, i.e. for each volt increased in the PCC, the voltage control is able to reduce it 1. The minimum value would be 0, corresponding to the reference case where no Volt-VAr control is applied. The number is obtained considering all the points that fulfills the following two conditions: the line voltage is higher than u_{max} and the reactive power less than Q_{min}.
- *95^{th} percentile voltage reduction (%)*: It indicates the voltage reduction that a specific Volt-VAr control is able to achieve. In order to better see its effectiveness, this value is expressed in relation to the maximum voltage deviation allowed by the standards (10% of the nominal voltage), ΔU_{max}=40V. The 95^{th} percentile value is taken instead of the maximum voltage value to avoid singular points, for example, when there is no reactive power availability the same maximum voltage values are obtained both in the reference and in the evaluation periods. This indicator would point out that for 95% of the test the values of voltage in the PCC kept below that number, matching, also, the EN50160 standard.
- *Line current increase (%)*: This indicator calculates the average line current for 5-day period when the voltage is higher than u_{max}, comparing the reference with the evaluation periods.
- *Power factor*: Is the ratio between the total active power and the total apparent power supplied by the inverter. When reactive power control is enabled, the total apparent power increases and, therefore, the power factor should reduce. Again, this indicator is calculated as the average for 5-day period when the voltage is higher than u_{max}.

4. Results

In this section, the results from the six tests are presented. The outcomes of the optimization process related to the overvoltage (droop, u_{max} and Q_{min}) for all tests are listed in table 3

Table 3. Summary of the optimized parameters for the six evaluation periods

Scenaio	Optimization mode	droop	u_{max} [pu]	Q_{min} [VAr]
1	M	5.789	1.001	-794
2	M	35.69	1.001	-2114
1	FV	1.000	1.005	-1694
2	FV	7.748	1.005	-4000
1	B	1.001	1.010	-2999
2	B	8.030	1.010	-1364

Lower droop indicates higher slope for the Volt-VAr curve, i.e. for each Volt increase in the PCC more reactive power will be absorbed by the PV inverter. In figure 7, the effectiveness of the droop parameter is plotted by scenario and optimization mode.

Preprints (www.preprints.org) | NOT PEER-REVIEWED | Posted: 26 February 2021 doi:10.20944/preprints202102.0595.v1

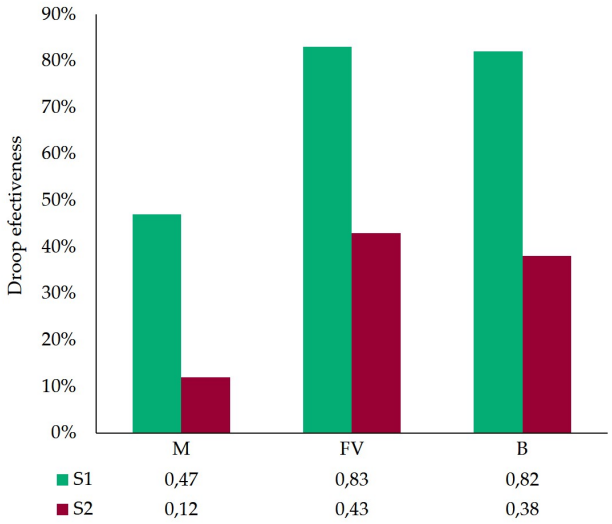

Figure 7. Droop effectiveness from evaluation periods of all tests

Lower values of droop mean that the Volt-VAr control is more effective, however, there are other parameters to consider. Later in section 5 the problems of taking low values of droop parameter in weak grid topologies are presented. Moreover, the effectiveness of the control relies on the actual voltage reduction it can achieve based on the grid topology where the PV inverter is located. In figure 8 the 95th percentile of the maximum voltage reduction in the PCC is indicated, relative to the maximum allowed deviation.

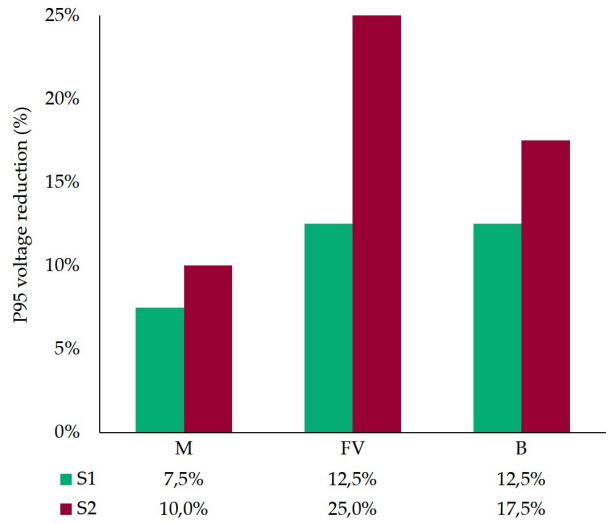

Figure 8. 95th percentile voltage reduction relative to maximum allowed deviation

Figure 8 shows how the parameters adapted to a weak topology grid, like in S2, so the control is able to reduce the voltage up to 25% of the maximum voltage deviation (10V), when there is more need for it, even though droop parameters in S2 were larger than in S1. Figure 9 plots the line voltage for a 5-day test for both the reference period of S2 and the evaluation of S2 with FV optimization mode. The voltage reduction of 25% can be perceived by looking at the straight lines.

Preprints (www.preprints.org) | NOT PEER-REVIEWED | Posted: 26 February 2021 doi:10.20944/preprints202102.0595.v1

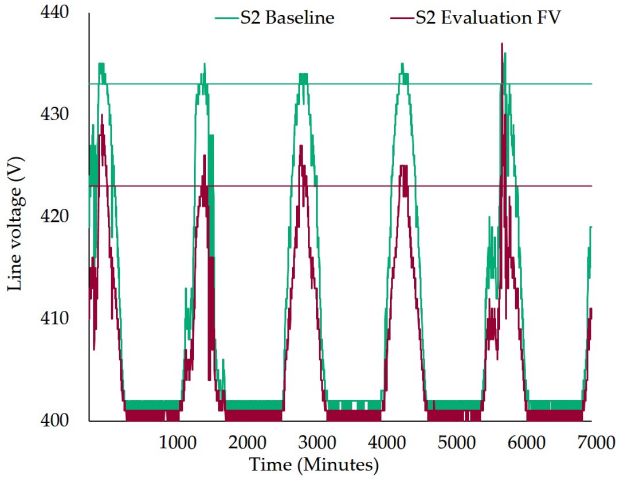

Figure 9. Line voltage for 5-day test. Straight lines indicate the 95^{th} percentile from the maximum voltage

The threshold of the reactive power that the PV inverter can absorb (Q_{min}) is another indicator of the effectiveness of the control since it allows for more voltage reduction. Lower thresholds of Q_{min} allow more reactive power control absorption and, therefore, more current flowing through the lines. Figure 10 Line current increase (%) from evaluation periods compared with reference periods for all tests. presents the line current increase when there is voltage regulation control.

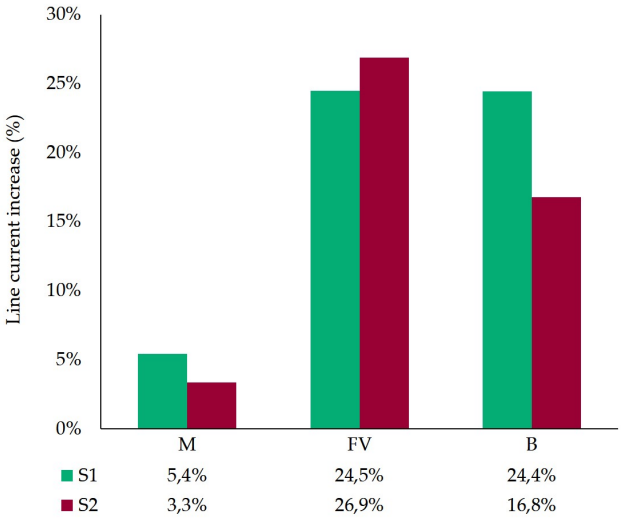

Figure 10. Line current increase (%) from evaluation periods compared with reference periods for all tests

Line current increase is also conditioned to the droop effectiveness, for that reason in the *mixed* optimization mode there is more line current increase in strong grid topology than in weak one even though the threshold is higher (Q_{min}=-794 VAr in S1 and Q_{min}=-2113 VAr in S2). However, lower values of Q_{min} lead to lower values of power factor, sometimes undesired for to proper operation of the grid. Figure 11 presents the power factor for all tests.

Preprints (www.preprints.org) | NOT PEER-REVIEWED | Posted: 26 February 2021 doi:10.20944/preprints202102.0595.v1

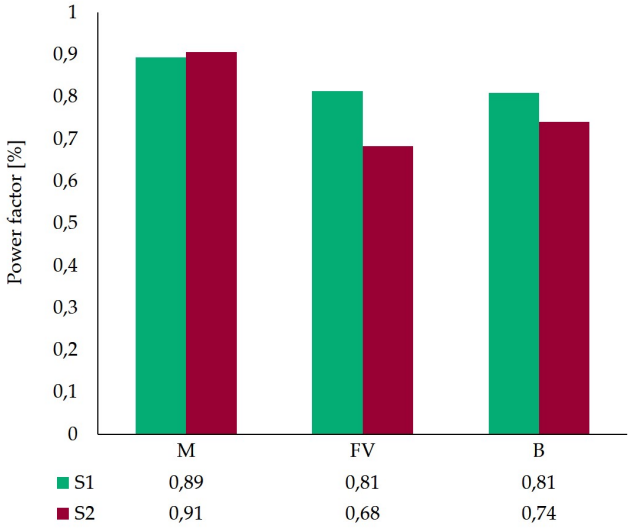

Figure 11. Average power factor for all 5-day evaluation periods when voltage in the PCC is above u_{max}

5. Discussion

5.1. Optimized Volt-VAr parameters

Volt-VAR control algorithm has been tested and its effectiveness proven. The *mixed* mode was the less efficient in terms of voltage reduction but the most conservative in terms of current increase. The *full voltage* mode was the one to achieve more voltage reduction in both scenarios and the *balanced* gives an intermediate solution between the previous two modes. Nevertheless, the results obtained are discussed and some recommendations on when each mode is suitable to use beyond voltage deviation and line current reduction are given.

A small droop parameter together with a low threshold of Q_{min} and u_{max} close to nominal voltage seems to be the best option to achieve higher voltage reduction. However, the tests show that small values of droop entail reaching the reactive power limit soon. In case this threshold is a low value (Q_{min} is negative), the PV emulator works at low power factor values most of the time. In this study, the power factor of the PV inverter has not been limited, but the fact that active power is priorized in front of reactive power, at high PV generation there is less reactive power availability as the active power reaches the nominal power of the PV inverter. Then, the voltage increases both for the unavailability of reactive power and for the increase of active power. This effect is represented in figure 12 where the dashed blue line represent the designed behaviour, as it was represented in figure 1.

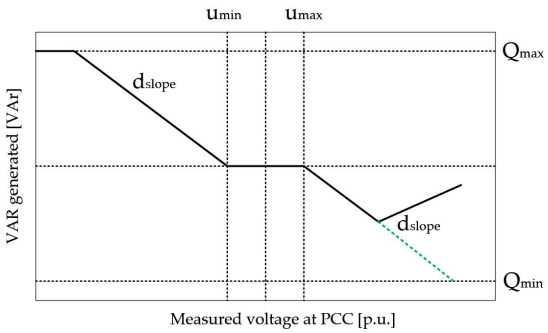

Figure 12. Effect on reactive power unavailability in Volt-VAr curve

The preferred optimization mode to avoid this effect will be the one that better fit the grid requirements: For weak grids with large PV penetration it might be preferred to use

Preprints (www.preprints.org) | NOT PEER-REVIEWED | Posted: 26 February 2021 doi:10.20944/preprints202102.0595.v1

higher values of Q_{min} (Q_{min} is negative), so there is enough reactive power availability when there is more active power generation. For example, reactive power limit in test 6 (S2, B) Q_{min}= 1364.974 VAr is bigger than in test 4 (S2, FV) Q_{min}= 3999.747 VAr. Then, in test number 6, less voltage reduction is achieved but there has been reactive power availability for almost all 5-day test, especially in moments of large active power generation, where voltage increase is particularly high, test 6 is preferred than test 4 in terms of grid stability. Thus, in those cases, it will be better to use the *balanced* optimization mode.
In case of both strong grids and weak grids with low penetration of PV and low line loadings, the preferred optimization mode would be the *full voltage* because it is the mode that provides more voltage reduction. In some cases, though, where the power factor of the loads is not inductive, the usage of *full voltage* mode will not be the recommended since the power factor would be lower than the recommended value.
The *mixed* optimization mode would be more useful in those lines highly loaded, especially in weak grids, where it is more important not to add more current to the power lines but still reduce the overvoltage.
The effect of the grid strength really matters when looking for a Volt-VAr control able to adapt to the grid topology where it is installed. Large values of reactance entail a voltage reduction while large values of resistance mean less voltage reduction. In the cases studied, the maximum voltage reduction is achieved in Test 4, the *full voltage* optimization mode for S2, with almost 25% (10V) compared to the maximum voltage deviation (40V).

5.2. Test design limitations in a microgrid laboratory

Working with real equipment in a microgrid laboratory lead to some limitations not present in analytical calculations or simulated environments. Some limitations challenged during the testing phase are listed below:

- *Unbalanced grid voltage*: Grid emulator's power electronics uses the direct-quadrature-zero transformation to simplify its control. This transformation should be used in balanced system; otherwise, the control will lead to undesired operation of the converter. Due to the unbalanced consumption of metering equipment, PV emulator and distribution line impedance, the control parameters in the grid emulator have been adjusted to compensate voltage grid unbalances.
- *Oscillating reactive power setpoint*: Voltage measurements from internal voltmeter in the PV emulator provide integer values to the control algorithm. Because of this integer data, the obtained reactive power setpoints in the laboratory environment might have a discontinuity, leading in some cases to an oscillating and inaccurate control. It was compensated by increasing the sampling time of the voltmeter.
- *Inaccurate closed loop control*: Internal closed loop control of active and reactive power of PV emulator was not accurate in the whole range of power. Even though the sensors are calibrated and the control adjusted, still there is up to 3% inaccuracy between setpoint and sensor measures.

5.3. Other power quality considerations

For all tests carried out, line current is very small compared to the maximum line capacity because the test has been designed for a system with only one power generation unit. Meanwhile the cable capacity is between 100 and 200 A, the maximum current provided by the PV emulator is around 5 A. Despite line loading is not an issue for these tests, the increase of current when using a reactive power control is proven. Power factor is the consequence of the active and reactive power that the control algorithm sets to the emulator, in some tests a value as low as 0.68 (Figure 11) is obtained in average for a 5-day test, which is not acceptable in terms of distribution grid recommendation. However, distribution lines are inductive and most of the loads too, then a capacitive reactive power behaviour of the emulator as the ones obtained in this study can compensate the typical inductive performance of electric grids.
THD must be less than 5% for general application according to previously mentioned

Preprints (www.preprints.org) | NOT PEER-REVIEWED | Posted: 26 February 2021 doi:10.20944/preprints202102.0595.v1

standards. The values remained within regulation limits and there is no correlation between the increase of THD and reactive power use of PV emulator. Figure 13 plots the THD and reactive power measured at each minute of evaluation period of Test 4.

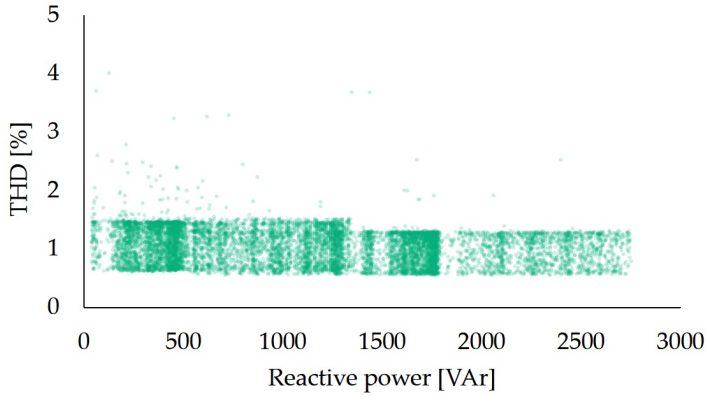

Figure 13. Correlation between reactive power and THD is almost 0

6. Conclusions

The effectiveness for voltage reduction of the adaptive Volt-VAr algorithm depending on the electrical network characteristics is proven with three different optimization modes. Considering PV penetration and line loading levels the results show which mode is more suitable to use in weak or strong grids:
The *balanced* optimization mode better fits weak grids with large PV penetration. The *full voltage* would be prefered in both strong grids and weak grids with low penetration of PV and low line loadings. The *mixed* optimization mode would be more useful in weak grids with highly loaded lines.
The outcomes of this study point out that a low value of droop parameter and reactive power thresholds are not always desired when looking for a large voltage reduction and fulfill what the regulation specify. Reactive power availability in PV inverters is discussed to be relevant and a capacitive power factor presents an advantage for usually inductive-driven grids. The microgrid laboratory offers an appropriate environment to integrate the RTU with PV systems and train the algorithm based on power meter data. Among the studied scenarios, a voltage reduction up to 25% of the allowed voltage deviation it is achieved while keeping THD within regulation limits. Such outcomes together with the possibility to use RTUs with a local or a centralized control appeals the network operator to enhance the grid stability for different grid topologies.
Currently, the optimized control algorithm is under evaluation in a real field test in the Lavrion Technological Park in Greece (NTUA) in the context of the SABINA project. Preliminary results indicate that the concept operates as expected, achieving more voltage reduction than the default voltage control of PV inverters.

Author Contributions: Conceptualization, William Martin, Yves Stauffer and Pierre-Jean Alet; Data curation, Toni Cantero Gubert; Formal analysis, William Martin and Yves Stauffer; Funding acquisition, Cristina Corchero; Methodology, Toni Cantero Gubert, Alba Colet, Lluc Canals Casals and Amelia Alvarez de Sotomayor; Supervision, Lluc Canals Casals, Cristina Corchero, Jose Luís Domínguez-García and Pierre-Jean Alet; Validation, William Martin and Yves Stauffer; Writing – original draft, Toni Cantero Gubert; Writing – review editing, Toni Cantero Gubert, Alba Colet, Lluc Canals Casals, Jose Luís Domínguez-García, Yves Stauffer and Pierre-Jean Alet. All authors have read and agreed to the published version of the manuscript.

Funding: The European Community Horizon 2020 program under project SmArt BI-directional multi eNergy gAteway (SABINA), grant agreement 731211, has financially supported this research.

Conflicts of Interest: The authors declare no conflict of interest.

References

1. Hu, Aixue; Levis, Samuel; Meehl, Gerald A.; Han, Weiqing; Washington, Warren M.; Oleson, Keith W.; van Ruijven, Bas J.; He, Mingqiong; Strand, Warren G. Impact of solar panels on global climate. *Nature climate change* **2016**, *6(3)*, 290–294.
2. Alet, P.J.; Baccaro, F.; De Felice, M.; Efthymiou, V.; Mayr, C.; Graditi, G.; Juel, M.; Moser, D.; Petitta, M.; Tselepis, S. and others. Quantification, Challenges and Outlook of PV Integration in the Power System: A Review by the European PV Technology Platform. In proceedings of the 31st European Photovoltaic Solar Energy Conference and Exhibition (EU PVSEC 2015), Hamburg, Germany, 14–18.
3. Chen, P.C.; Salcedo, R.; Zhu, Q.; De Leon, F.; Czarkowski, D.; Jiang, Z.P.; Spitsa, V.;Zabar, Z.;Uosef, R.E. Analysis of voltage profile problems due to the penetration of distributed generation in low-voltage secondary distribution networks. *IEEE Transactions on Power Delivery* **2012**, *27(4)*, 2020–2028.
4. Mahmud, N; Zahedi, A. Review of control strategies for voltage regulation of the smart distribution network with high penetration of renewable distributed generation. *Renewable and Sustainable Energy Reviews* **2016**, *64*, 582–595.
5. Delgado-Gomes, V.; Martins, J. F.; Lima, C.; Borza, P. N. Towars the use of Unbundle Smart Meter for advanced inverters integration. In proceedings of the IEEE 26th International Symposium on Industrial Electronics (ISIE), Edinburgh, UK, 2017.
6. CENELEC. EN 50438 Requirements for micro-generating plants to be connected in parallel with public low-voltage distribution networks. Brussels, 2013.
7. CENELEC. EN 50160 Voltage characteristics of electricity supplied by public distribution systems. Brussels, 2010.
8. Eltawil, M. A.; Zhao, Z. Grid-connected photovoltaic power systems: Technical and potential problems - A review. *Renewable and Sustainable Energy Reviews* **2010**, *14(1)*, 112–129.
9. Subburaja, A. S.; Shamim, N.; Bayne, S.B. Battery connected DFIG wind system analysis for strong/weak grid scenarios. In proceedings of the 2016 IEEE Green Technologies Conference (GreenTech), 112–117.
10. Seuss, J.; Reno, M.J.; Broderick, Robert J.; Grijalva, S. Analysis of PV Advanced Inverter Functions and Setpoints under Time Series Simulation. Sandia National Laboratories, Albuquerque, New Mexico, 2016
11. Miranda, T.; Delgado-Gomes, V.; Martins, J. On the use of IEC 61850-90-7 for Smart Inverters Integration. In proceedings of the 2018 International Conference on Intelligent Systems (IS). Funchal, Portugal, 2018. 722–726
12. Alet, P.-J.; Adinolfi, G.; Barchi, G.; Bründlinger, R.; Graditi, G.; Henze, N.; Jung, M.; Stavrou, A.; Yang, G. The Inverter: A Multi-Purpose Control Element. In proceedings of the 36th European Photovoltaic Solar Energy Conference and Exhibition, 2019.
13. Yang, D.; Wang, X.; Liu, F.; Xin, K.; Liu, Y.; Blaabjerg, F. Adaptive reactive power control of PV power plants for improved power transfer capability under ultra-weak grid conditions. *IEEE Transactions on Smart Grid* **2019**, *10(2)*, 1269–1279.
14. Kim, Y.-S.; Kim, G.-H.; Lee, J.-D.; Cho, C. New Requirements of the Voltage/VAR Function for Smart Inverter in Distributed Generation Control. *MPDI Energies* **2016**, *9(29)*, 1–14.
15. Takasawa, Y.; Akagi, S.; Yoshizawa, S.; Ishii, H.; Hayashi, Y. Effectiveness of updating the parameters of the Volt-VAR control depending on the PV penetration rate and weather conditions.In proceedings of the IEEE Innovative Smart Grid Technologies - Asia, Auckland, 2017
16. Santos-Martin, D.; Lemon, S. Simplified Modeling of Low Voltage Distribution Networks for PV Voltage Impact Studies. *IEEE Transactions on Smart Grid* **2016**, *7(4)*, 1924-1931.
17. Li, S.; Sun, Y.; Ramezani, M.; Xiao, Y. Artificial Neural Networks for Volt/VAr Control of DER Inverters at the Grid Edge. *IEEE Transactions on Smart Grid* **2019**, *10(5)*, 5564-5573.
18. Martin, W.; Stauffer, Y. SmArt BI-directional multi eNergy gAteway (SABINA) - Deliverable D3.2: Supervisory layer for inverter control validated. The European Commission, 2018.
19. Fawzy, T. F.; Bletterie, B.; Deprez, W.; Buelo, T.; Bettenwort, G.; Engel, B. "New strategies for coordinated control in power distribution grids — Effective integration of photovoltaic plants utilizing sensitivity analysis," in 48th International Universities' Power Engineering Conference (UPEC), Dublin, Ireland, 2013.
20. Demirok, E.; Pablo, C. G.; Sera, D.; Rodriguez, P.; Teodorescu, R. "Local Reactive Power Control Methods for Overvoltage Prevention of Distributed Solar Inverters in Low-Voltage Grids," IEEE Journal of Photovoltaics, vol. 1, no. 2, pp. 174 - 182, 2011.
21. Taddeo, Paolo; Colet, Alba; Carrillo, Rafael E.; Casals Canals, Lluc; Schubnel, Baptiste; Stauffer, Yves; Bellanco, Ivan; Corchero Garcia, Cristina; Salom, Jaume. *Energies* **2020**, *13(5)*
22. Marzband, M.; Sumper, A.; Ruiz-Álvarez, A.; Domínguez-García, J.L.; Tomoiaga, B. "Experimental evaluation of a real time energy management system forstand-alone microgrids in day-ahead markets," *Applied Energy***2013**, p. 365–376.
23. Schneider Electric, "https://www.se.com," [Online]. Available: https://www.se.com/ww/en/product-range-download/62685-saitel-dr-remote-terminal-unit-%26-controller/#/documents-tab. [Accessed 10 01 2020].